DOPPLER SODAR AND ATMOSPHERIC BOUNDARY LAYER DETECTION

Zhou Mingyu (周明煜), *Chen Jingnan* (陈景南), *Li Shiming* (李诗明), *Zheng Yueming* (郑月明), *Su Lirong* (苏立荣) and *Lü Naiping* (吕乃平)

National Research Center for Marine Environment Forecasts, State Oceanic Administration, Beijing

Received November 8, 1990

ABSTRACT

A Doppler sodar system controlled by microcomputer is described in this paper. The sodar was used to detect the vertical distribution of wind and temperature stratification in the atmospheric boundary layer. The detecting results show that at night the vertical distribution of wind is very complicated, which can appear as a structure of two or three layers. In nocturnal atmospheric boundary layer sometimes there exists very thin layer in multi-layer inversion and it can be retained for a long time.

Key words: Doppler sodar, atmospheric boundary layer, wind measurement, multi-layer inversion

I. INTRODUCTION

The Doppler sodar is an important method for remote sensing of the atmospheric boundary layer. In 1969, Australian scientist McAllister first successfully made a sodar system. Since then much research work has been carried out by many scientists, such as Mandics et al. (1975) and Spizzichino (1974). Chinese scientists (Zhou et al.,1980, 1981; Lü et al., 1988, 1989) analyzed the characteristics of atmospheric boundary layer over land and ocean by using monostatic acoustic radar.

It is very important to measure the wind velocity and temperature structure in the boundary layer atmosphere for studying the air-sea interaction and air pollution. The low level wind shear has a direct effect on airplane flying safety and missile launching. Therefore, in recent three years we have developed a new type of Doppler acoustic radar for studying the structure of atmospheric boundary layer over land and ocean. It is also applied in real-time monitoring of environmental protection and nowcasting of military and civil aviation.

II. FUNDAMENTAL DETECTING PRINCIPLE

A sound pulse is transmitted vertically upward to the atmosphere by an acoustic radar. The sound pulse propagates upward with a sound speed. The scattering of sound wave can be induced by the inhomogeneous distribution of atmospheric wind speed and temperature, but the backscattering is only related with the inhomogeneity of temperature. The echo power can be expressed as a scattering formula

$$P_r = \eta_t \eta_r A_r P_T \sigma(r, f) \frac{C\tau}{2} \frac{1}{h^2} L, \qquad (1)$$

where P_r is the received echo power; P_T the transmitted electrical power; η_t and η_r are conversion

efficiencies for electrical to acoustic and acoustic to electrical power respectively; A_r is the effective receiving antenna area; $\sigma(r.f)$ the backscattering cross section; C sound speed, τ the transmitted pulse width, h the height of sound scatter, and L an attenuation factor. From Eq. (1) we can see that when the parameters of an acoustic radar system are defined the received echo power is directly proportional to the backscattering cross section σ and is inversely proportional to the square of the scatter height. Since $\sigma \propto (dT/dh)^2$, here T is atmospheric temperature,and dT/dh is temperature gradient, the echo power is proportional to the square of temperature gradient and the amplitude of the echo electric voltage is proportional to the absolute value of temperature gradient. Therefore, according to the variation of echo intensity in time and space, the temporal and spatial distribution of temperature gradient can be obtained.

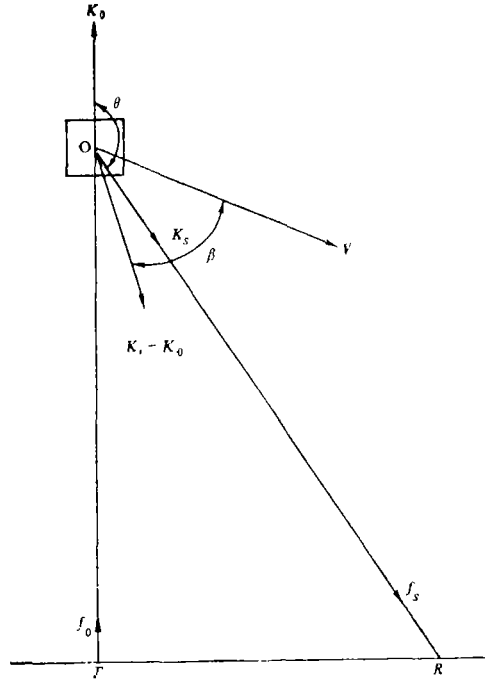

Fig. 1. Detecting principle for measuring wind with acoustic radar.

Doppler effect can be caused by the wind velocity in the atmosphere and corresponding Doppler shift between the transmitted frequency and received echo frequency is then produced. The Doppler principle is also used in acoustic remote sensing and the fundamental detecting principle was suggested by Clifford (1974) as shown in Fig.1. A sound pulse with a frequency f_0 is transmitted vertically upward from antenna T. At point O there is a scattered volume moving with the wind velocity V. Owing to the Doppler effect, at antenna R the received echo frequency becomes f_s, the frequency deviation is $\Delta f = f_s - f_0$. The value of Doppler frequency shift is proportional to wind velocity $\boldsymbol{V}$. If $\boldsymbol{K}_0$ is a wave vector of the transmitted acoustic wave and $\boldsymbol{K}_s$ is the wave vector of the scattered acoustic wave, the Doppler frequency shift can be expressed as

$$\Delta f = \frac{1}{2\pi}(\boldsymbol{K}_s - \boldsymbol{K}_0) \cdot \boldsymbol{V} \ , \qquad (2)$$

where $\boldsymbol{V}$ is a wind velocity vector on a plane, constructed by transmitted and received beams. In Fig. 1, if the scattered angle θ and angle β constructed between vectors $\boldsymbol{V}$ and $\boldsymbol{K}_s-\boldsymbol{K}_0$ are known, from Eq. (1) Δf can be derived,

$$\Delta f \simeq -\frac{2|\boldsymbol{V}|}{\lambda_0}\cdot \sin(\theta/2)\cos\beta, \tag{3}$$

where $\lambda_0 = C/f_0$, C is sound velocity. Then we have

$$|\boldsymbol{V}|\cos\beta = V' = \frac{C}{2}\sin(\theta/2)\cdot\left(\frac{\Delta f}{f_0}\right). \tag{4}$$

It means that the measured wind vector is along the direction of $\boldsymbol{K}_s-\boldsymbol{K}_0$. If a same antenna is used for both transmitting and receiving, so-called monostatic antenna system ($\theta=180°$), Eq. (4) then becomes

$$V' = \frac{C}{2}\left(\frac{\Delta f}{f_0}\right). \tag{5}$$

The measured wind vector is along the radial direction of antenna beam.

In order to measure the total wind vector, a three-antenna system is used. Three antennas are set in two planes which are perpendicular each other as shown in Fig.2a. Two antennas

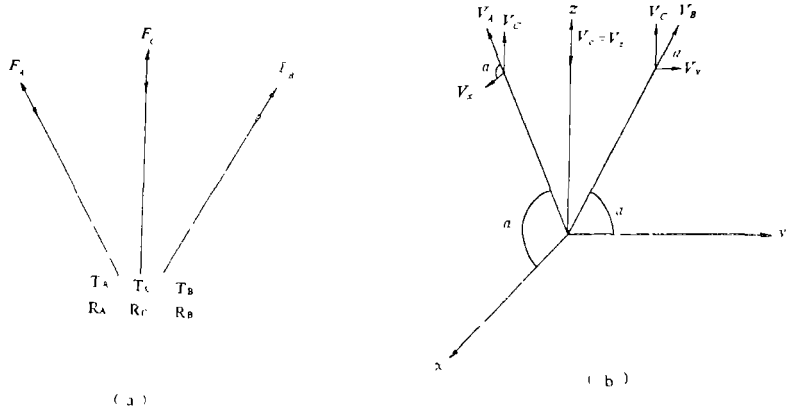

Fg. 2. Antenna system configuration and principle of measuring wind.

T_A and T_B are inclined, with an angle α to horizontal direction. Antenna Tc is vertically pointed. These three antennas used simultaneously for transmitting and receiving, with a transmitted frequency f_0, the radial wind velocities are

$$\begin{aligned} V_a &= -\frac{C}{2}\left(\frac{\Delta f_a}{f_0}\right), \\ V_b &= -\frac{C}{2}\left(\frac{\Delta f_b}{f_0}\right), \\ V_c &= -\frac{C}{2}\left(\frac{\Delta f_c}{f_0}\right), \end{aligned} \tag{6}$$

where sign minus"–" represents that the wind direction is opposite to the sign of Δf, i.e. when $\Delta f>0$, the air flow moves down along the axis; while $\Delta f<0$, upward. Form Fig. 2b we can easily obtain

$$V_x=(V_a-V_c\sin\alpha)/\cos\alpha,$$
$$V_y=(V_b-V_c\sin\alpha)/\cos\alpha, \quad (7)$$
$$V_z=V_c.$$

The total wind vector can be written as

$$\boldsymbol{V}=V_x\boldsymbol{i}+V_y\boldsymbol{j}+V_z\boldsymbol{k}. \quad (8)$$

According to the ratio of V_x to V_y and its sign the wind direction can be defined .

III. THE CONFIGURATION OF DOPPLER SODAR SYSTEM

The Doppler sodar system consists of antenna, transmitter, receiver, antenna switch, PC/386 microcomputer, FFT board and other external devices. The system diagram is shown in Fig.3.

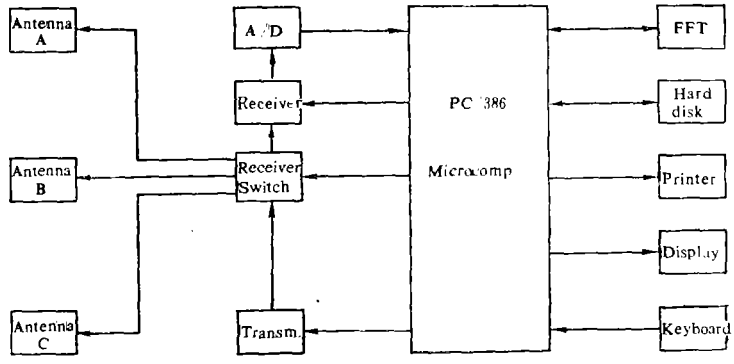

Fig. 3. Doppler acoustic radar system diagram.

(1) Sodar antenna consists of a flat trailer, parabolic reflector, absorbing foam and transducer. The parabolic reflector with a diameter of 1.2m and a screen around the antenna for attenuating the sound noise are made from fiber glass. The working frequency is at 1600Hz.

(2) The main part of Doppler sodar consists of transmitter, receiver, T-R transit switch and power supply. The PC/386 microcomputer controls three antennas (A,B,C) working in turn through T-R transit switch. The transit cycle can be selected between 6—90 seconds, and the corresponding transit cycle for each antenna is 2—30 seconds. The transmitter and receiver complete transmitting the sound pulse and extracting echo signal respectively.

(3) PC/386 microcomputer has 640KB RAM, Great-Wall EGA card and color display terminal, and 80MB hard disk. DOS 3.3 operating system can support operating Assembly, Fortran, and Basic languages.

(4) A/D conversion board is a multifunction A/D board with 32-channel analog input and 2-channel analog output. It has a resolution of 12-bit ,32-channel DI/O and 4-channel 16-bit timer/counter.

(5) FFT board is one of the main parts of this system. By use of TMS 32020 VLSI signal processing chip, it takes only 42 ms for 1024 point complex FFT operation. The spectrum analysis of Doppler signals and the frequency shift detection are conducted with the board.

(6) This system is equipped with an M1570 color printer. As output equipment used for copying the data of wind speed and echo diagram, it can clearly show the diagram of echo intensity which varies with height and time, and the profiles for wind speed and direction.

(7) The accuracy of the Doppler sodar measurements is 0.3 m/s in horizontal wind

speed, 0.05m/s in vertical, and $\pm 3°$ in wind direction. The measured wind speed ranges from 0 to 28 m/s, and detection height from 30 to 1000m. A comparative experiment has been done at Nanyuan airport by using Doppler sodar, three-component anemometer and ADAS tethersonde. Shown in Fig.4 is a correlation diagram for the comparison. The variance of wind velocity is 0.5, which is calculated from the wind velocity deviation between sodar and three-component anemometer based on 177 samples, the variance of wind direction deviation is 14.13, and the variance of vertical velocity deviation is 0.15. On the other hand, the variance of wind velocity is 0.54 which is calculated from the deviation between Doppler sodar and tethersonde based on 46 samples, and the variance of the wind direction deviation is 25.92. Two examples of profiles for wind velocity and direction measured by sodar and ADAS tethersonde shown in Fig.5 indicate that these results are very close each other.

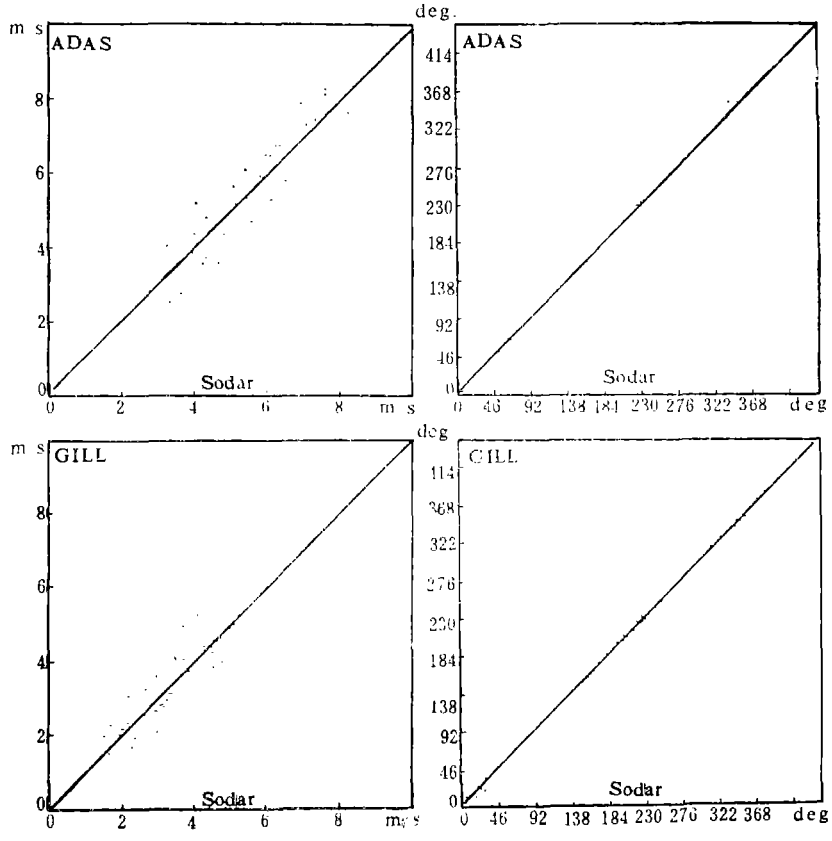

Fig. 4. The correlation of winds measured with sodar, three-component anemometer and ADAS system. (Mar. 9—12, 1989)

In order to make a comparison of the experimental results mentioned above with that in foreign countries, the results of comparative experiments carried out at Boulder CO U.S.A. are shown in Table 1. The Doppler sodars made in four companies were compared at BAO station in Boulder, and the comparative experiment was conducted in 1982 and supported by Wave Propogation Laboratory,NOAA, U.S.A. The results listed in Table 1 show that the results of our comparative experiment are in agreement with that in Boulder experiment.

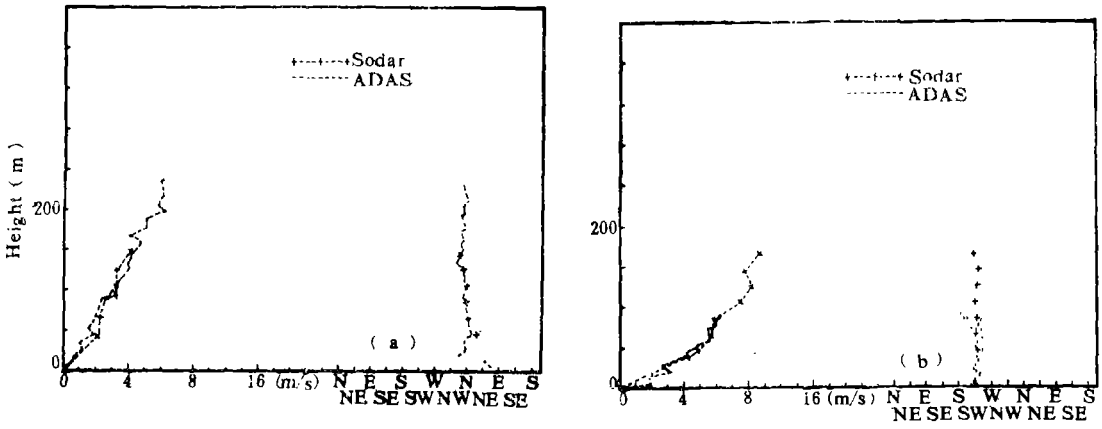

Fig. 5. A Comparison of wind profiles measured with sodar and ADAS system. (a) 0150 BT Dec.3, 1989, (b) 2210 BT Dec. 3, 1989.

Table 1. A Comparison of Wind Speeds Measured with Sodar and Sonic Anemometer on BAO Tower at 200 m Height

Type of sodar	Wind speed		Wind direction		Vertical speed	
	n^*	VD^{**}	n^*	VD^{**}	n^*	VD^{**}
(1200—1700BT)						
Aerovironment	69	1.33	69	19.69	45	0.31
Remtech	44	0.91	44	30.69	35	0.15
Radian	64	1.91	64	18.25	37	0.32
Xontech	67	1.93	67	29.24	32	0.38
(0000—0500BT)						
Aerovironment	59	0.62	59	19.29	25	0.16
Remtech	41	0.42	41	11.65	20	0.10
Radian	53	0.88	53	24.31	27	0.22
Xontech	63	0.87	63	34.45	27	0.22

$^*n$: sample number
$^{**}VD$: the variance of deviation

IV. ANALYSIS OF OBSERVATIONAL RESULTS

A Doppler sodar is set in the courtyard of a storehouse which is situated in northwestern suburb of Beijing and attached to State Oceanic Administration. The storehouse is 70 meters above sea level. About 5 km north of the storehouse rises a mountain of Jiansanzui, 700m above sea level, to west of the storehouse is Shuanglongling, further west there is a mountain, 1000m above sea level. To the east of the storehouse the plain stretches out and the terrain in the south of the storehouse slopes gently. 8 to 9km south of the storehouse there are some hills. Continuous detection of the vertical distribution of wind and temperature stratification in the atmospheric boundary layer was carried out by using the Doppler Sodar.

Because the observational site (the storehouse) is near mountain area, obvious local wind characteristics are present under the weak wind weather. When the weather is controlled by severe weather systems, they are not so obvious. Below we will analyze the vertical charac-

teristics of local wind under weak wind weather. On the 700 hPa weather map of 2000 BT 24 May, Beijing is situated in the rare of trough. On the simultaneous surface weather map, the eastern China is controlled by a high pressure, the surface wind is very weak, Beijing is on the left side of the high pressure and southwest wind prevails. On the surface weather map of 0200 BT 25 May, it is calm and still controlled by a high pressure; and at 0800 BT

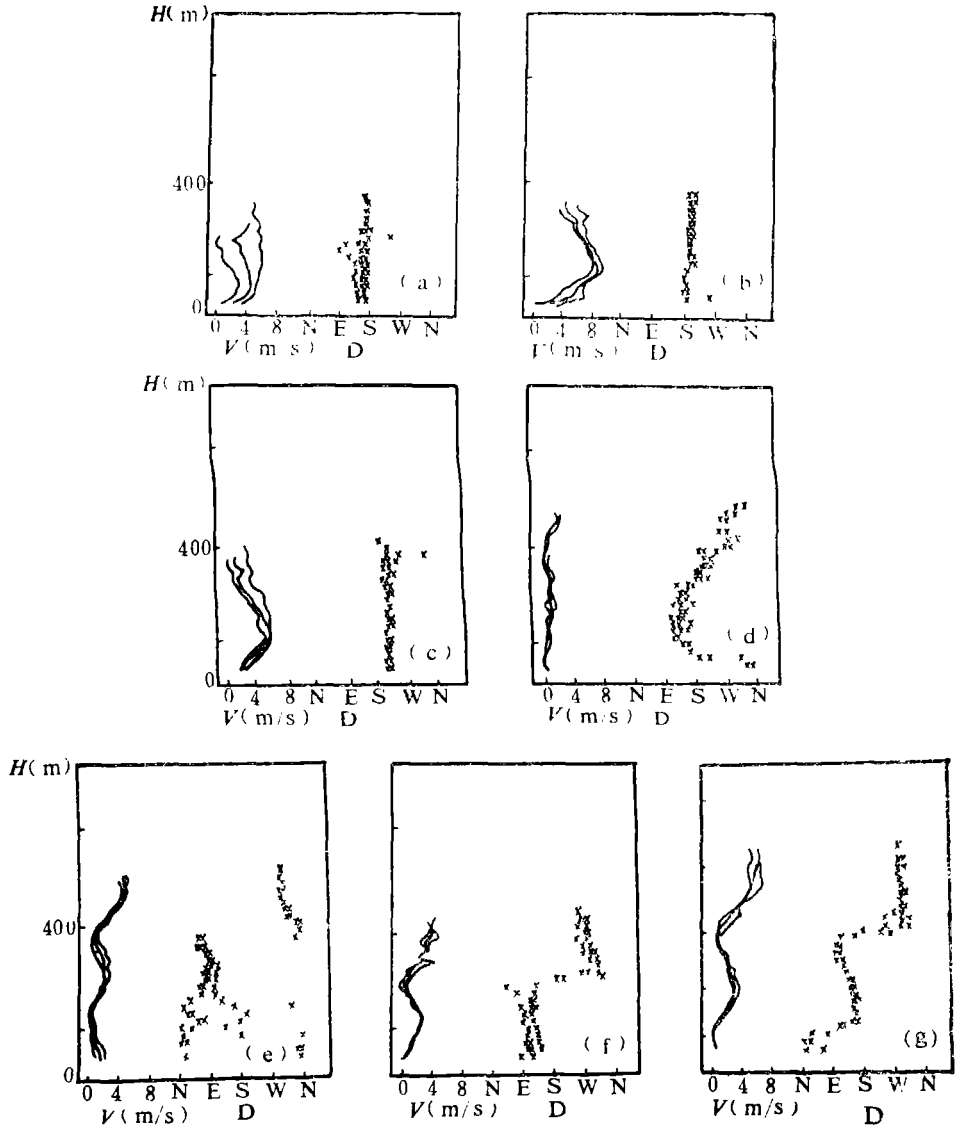

Fig. 6. The vertical distribution of the wind detected with the Doppler sodar (May 24—25, 1989).

southwest wind prevails with speed 2 to 4m/s. In the conditions as described above, it was clear in Beijing area. Therefore in the condition of weak wind, the local wind and inversion formed due to radiation cooling play an important role. In calm night and weak wind condition, the pollutants are difficult to diffuse, resulting in serious air pollution. Notice that, in this

case the local wind induced by the terrain will appear as a good atmospheric condition which may be beneficial to diffusion of pollutants. Therefore, study on the effect of local wind and inversion is important.

In the afternoon on May 24, detection results of the Doppler sodar showed that in the lower atmosphere below 400m the wind blows from the south with velocity 4—6m/s between 100 to 400m. Below 100m there exists a wind shear layer. Because the cooling induced by terrain is complex, the distributions of wind are different from that in flat area.

The observational results also showed that after 1700 BT an inversion layer appeared at 200m height and the wind velocity there gradually increased. A detecting result of Doppler sodar from 1730 to 1800 BT is given in Fig. 6b, showing that a maximum wind velocity larger than 8m/s appears at level 170m, and it is colse to the velocity of low-level jet. This indicates that near the mountain area the maximum wind velocity or low-level jet in the lower atmosphere may appear before sunset, which is different from the situation in flat area.

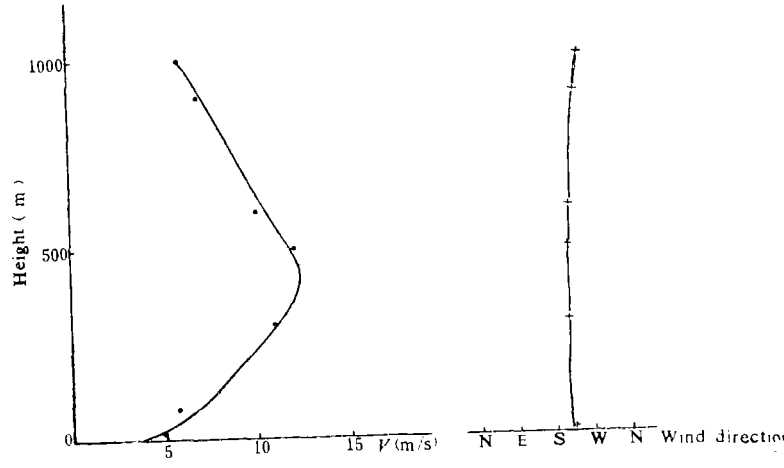

Fig. 7. The vertical distribution of wind detected at Beijing Meteorological Observatory. (1900 BT 24 May 1989)

Fig.7 is the vertical distribution of wind measured at Beijing Meteorological Observatory at 1900 BT 24 May. It can be seen from Fig.7 that in the atmospheric boundary layer the southerly wind prevails below 1 km. Near the height of 350m there is a low level jet with a maximum velocity of 12m/s. The geostrophic wind is 8.2m/s estimated from surface pressure gradient at 2000 BT 24 May. The 1900 BT radiosonde data measured at Beijing Meteorological Observatory showed that the lower atmosphere is under the stable condition. Therefore it is easy to understand the above fact that the low-level jet is larger than the geostrophic wind.

The observational results detected with Doppler sodar at the storehouse shown in Fig.6c illustrate a maximum southern wind velocity of 6m/s at level 160m in the wind profile at 1900 BT. Comparing Fig.7 with Fig.6c, we can see that the southwesterly wind prevails above the storehouse and Beijing Meteorological Observatory. But the wind velocity measured at the storehouse is obviously lower than that measured at Beijing Meteorological Observatory and the height of maximum wind speed at the storehouse is about 180m lower than that at Beijing Meteorological Observatory. It may be explained that the southern wind produced by the weather system decreases due to the increasing of terrain resistance effect as entering

into the mountain area. In addition, in the north and west of the storehouse, the drainage flow induced by radiation cooling of the mountain declivity can balance a part of south wind. Therefore it will decrease the southern wind which is controlled by the weather system. The height of maximum wind velocity at the storehouse is different from that at Beijing Meteorological Observatory. The elevation of Beijing Meteorological Observatory is 55m, and it is only 15m lower than the elevation of storehouse.Seemingly, the vertical inhomogeneity of the drainage flow may be the main cause for the height differences of the maximum wind velocity at two stations. In fact, the wind velocity is weak at the level of 300m above the storehouse. It means that the drainage flow is strong above 300m height. The corresponding detection of temperature stratification with sodar also illustrates that the strong inversion layer exists near 300m.

In the mountain area the drainage flow is gradually increasing with time. A vertical wind profile detected with sodar is shown in Fig.6d. Below 400m the wind velocity is weak, only 2m/s, the wind is from south in the layer between 100 to 150m. The wind direction becomes west and northwest near surface layer and above 300m. After midnight, the system wind gradually decreases, and on the surface weather map at 0200 BT, it is calm in Beijing area. At this time, the terrain wind prevails over the northwestern mountain area of Beijing.The wind distribution with three-layer structure usually appears above the storehouse. From Fig. 6e it is seen that the north wind appears below 150m, northeastern wind between levels 150 to 400m, and northwest wind above 400m. The wind velocity is 2m/s below 400m, and it increases gradually to 6m/s above 400m. The three-layer structure of the wind distribution is in correspondence with the inversion distribution The lowest inversion appears below 150m, and the top of strong echo layer of upper inversion is close to 400m.

After 0300 BT the systematic south wind recovers gradually. The north wind prevails in the upper and lowest layers and south wind appears in middle layer. Fig.6f gives the vertical distribution of the wind with typical three-layer structure. Northwestern wind appears above 400m, southeastern wind between 100m and 350m, and north wind below 100m. The change of wind direction is very quick between layers, i.e. the transition layer of wind direction is very thin, and the wind shear is strong. The multiple layer structure also can be seen in the vertical distribution of wind speed. The wind is weak below 100m and increases gradually with height above 100m, and reaches maximum value at 250m. Then the wind speed decreases gradually with height above 400m. This type of wind distribution is maintained until 0600 BT. This vertical structure of wind velocity may be formed by the overlapping of systematic southern wind on down slope wind induced by the mountain slopes at different heights in the complex mountain area. The northwestern wind above 400m may be correlated with the systematic wind at upper boundary layer. The down slope wind from northwest induced by the terrain is consistent with the systematic wind, and contributes to downward extension of northwestern wind. It may intensify the wind shear between the layer with northwest wind and the layer with south wind below 400m. After 0600 BT, because the slope surface is heated by the solar radiation, the northern wind in surface layer below 100m vanishes gradually and changes to southern wind. The observational data of Beijing Meteorological Observatory at 0700 BT show that it is calm on the ground and the northern wind prevails in upper layer. The detection of Doppler acoustic radar at 0700 BT at the storehouse shows (see Fig.6g) that there is eastern/southeastern wind below 250m and northwestern wind above 300m, and an obvious wind shear layer appears between 250m and 300m. Correspondingly the data of the vertical distributions of wind velocity show a clear two-layer structure. There is a

minimum value of wind speed near 300m. The southern wind is maintained until 0900 BT in the lower layer below 200m. After that, as the systematic northwestern wind increases, the whole boundary layer is controlled by the northwestern wind.

The nocturnal multi-layer inversion is also a notable problem .A result detected with sodar on December 21, 1988 presented that there was a typical process of multi-layer inversion. In the night of December 21, Beijing was controlled by a high pressure, the wind with northern direction was very weak. After sunset, a surface radiation inversion layer formed, then a multi-layer inversion gradually formed. Fig.8 is an example of observation at the building top of National Research Center for Marine Environment Forecasts, western suburb of Beijing. Although the nocturnal multi-layer inversion has been discussed by many scientists (such as Lü et al., 1988), but in this example, we have to point out that there is a thin stable echo layer between 100m and 200m. This layer is very thin, and almost maintained in whole night. Especially, it is clearly shown with a color terminal. As shown in Fig.8, there is a stable layer at level 150m, the depth of this echo layer is about 10m.Sometimes the depth of the echo layer may be larger than 10m, about 20 to 30m. This layer has a clear edge. In some cases an obvious wave with billow structure as shown in Fig.8a exists on this stable layer. The amplitude of this wave could reach 200m. Even so, the strong wave activity could not break the thin stable layer. In a stable atmosphere, although the turbulent intensity is very weak, the turbulence with certain intensity still exists. Even in the lower atmosphere with very stable stratification the intermittent turbulence could be formed by the interaction between the radiation cooling and wind shear in the surface layer (Zhou et al., 1982). Why the turbulent movement even the wave with large amplitude could not break the thin stable layer? What physical process could produce and maintain this thin stable layer for a long time? It is certainly a valuable subject for future research.

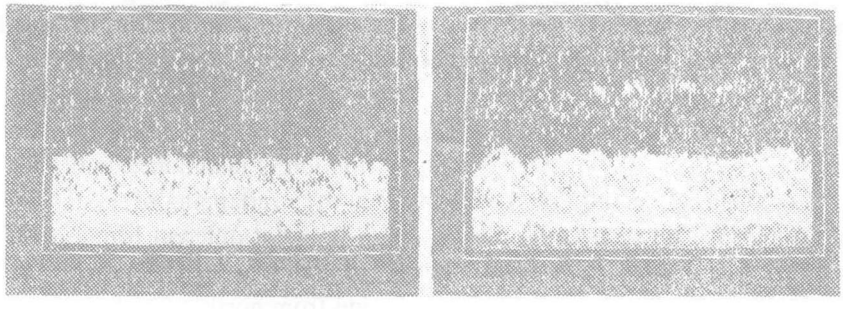

Fig. 8. The temperature structure detected with sodar (Dec. 22, 1988).

V. CONCLUSION

The Doppler sodar developed by us has high resolution, so we can obtain the structure of wind shear layer and the inversion structure in detail.

The observational results as described above are shown as follows:

(1) Near the Western Mountain area of Beijing, the low-level jet or a maximum wind

value in lower atmosphere may appear before sunset.

(2) The vertical distribution of wind in the lower atmosphere is very complicated near Western Mountain area of Beijing, it may present two or three-layer structure. At night, when the systematic wind is from south, the south wind appears in the middle layer, but in the upper and lower layers the north wind appears, the transition layer between layers with different wind directions is very thin.

(3) According to the sodar detecting data, sometimes there is a very clear and thin stable layer in the multi-layer inversion, and it can exist for long time. But its formation process is unknown, much research has to be done in the future.

REFERENCES

Clifford, S.F. and Brown, E.H. (1974), Acoustic scattering from a moving turbulent medium, *J. Acoustic Soc. Amer.*, **55**: 929—933.

Lü Naiping, Zhou Mingyu, Su Lirong and Chen Yanjuan (1988), A statistical analysis of sodar data detected in Yanshan area, Beijing, *Acta Meteor .Sinica,* **46**: 113—119 (in Chinese).

Lü Naiping, Li Shiming, Chen Jingnan, Zhen Yueming and Zhou Mingyu (1989), A calculation method of the sens'ble heat flux by sodar, *Acta Oceanologica Sinica,* **3**: 645—652.

McAllister, L.G. (1968), Acoustic sounding of the lower troposphere, *J.Atmos. Terr. Phys.*, **30**: 1439—1440.

Mandic, P.A. and Owens, E.J. (1975), Observations of the marine atmosphere using a ship-mounted acoustic echo sounder, *J. Appl. Meteor.*, **14**: 1110—1117.

Spizzichino, A. (1974), Discussion of the operating conditions of a doppler sodar, *J. Geophys. Res.*, **79(36)**: 5585—5591.

Zhou Mingyu, Lü Naiping and Chen Yanjuan (1980), The detection of the temperature coefficient of the atmospheric boundary layer by acoustic radar, *J. Acoustic Soc. Am.* **68(1)**: 303—308.

Zhou Mingyu, Lü Naiping, Chen Yanjuan and Li Shiming (1981), The lump structure of turbulence field in atmospheric boundary layer, *Scientia Sinica,* **24**: 1705—1716.

Zhou Mingyu and Zhang Yi (1982), The wave properties in process of the nocturnal radiative inversion, *Kexue Tongbao*, **27**: 156—159 (in Chinese).